Scale-free networks of earthquakes and aftershocks

Marco Baiesi[1,2] and Maya Paczuski[2,*]
[1]*INFM–Dipartimento di Fisica, Università di Padova, I-35131 Padova, Italy*
[2]*Mathematical Physics, Department of Mathematics, Imperial College London, London SW7 2BZ, United Kingdom*
(Received 15 October 2003; published 2 June 2004)

We propose a metric to quantify correlations between earthquakes. The metric consists of a product involving the time interval and spatial distance between two events, as well as the magnitude of the first one. According to this metric, events typically are strongly correlated to only one or a few preceding ones. Thus a classification of events as foreshocks, main shocks, or aftershocks emerges automatically without imposing predetermined space-time windows. In the simplest network construction, each earthquake receives an incoming link from its most correlated predecessor. The number of aftershocks for any event, identified by its outgoing links, is found to be scale free with exponent $\gamma=2.0(1)$. The original Omori law with $p=1$ emerges as a robust feature of seismicity, holding up to years even for aftershock sequences initiated by intermediate magnitude events. The broad distribution of distances between earthquakes and their linked aftershocks suggests that aftershock collection with fixed space windows is not appropriate.

DOI: 10.1103/PhysRevE.69.066106 PACS number(s): 89.75.Hc, 05.65.+b, 91.30.Dk

I. INTRODUCTION

Earthquakes exhibit complex correlations in space, time, as well as magnitude [1–6]. Sequences of earthquakes often appear related to main shocks of large magnitude, which are followed in time by nearby smaller events. Sometimes, the main shock is also preceded by a few intermediate or smaller precursor events. Earthquakes can also cluster as swarms, where the seismic activity is not distinctly associated with a main event. Human observation tends toward labeling these events depending on their relative magnitude and their position in the space-time sequence: foreshocks, main shocks, and aftershocks, respectively. However, in defining aftershocks, it is clearly necessary to distinguish them from what is called background seismicity, and to assign to each one its correct main shock(s). Although an observation by eye of the evolving seismic situation can support a classification, a precise label for each event may be intrinsically impossible.

In the most popular approach, aftershocks are collected by counting all events within a predetermined space-time window [7–10] following a main event (see Fig. 1), where both the main event and the space-time window are chosen *a priori* by the observer. Of course, the identification of aftershocks will change by altering the space-time window. Also, the method does not define the probability that an event thereby collected is actually correlated to the main event under consideration. Maybe more importantly, one does not know whether the selected space-time windows are too large or too small for minimizing errors in the procedure. A more subtle issue is to define aftershocks of aftershocks. If an aftershock can have more than one preceding large event, which of these should be regarded as the most important or correlated one? These remarks point to a fundamental question: are aftershocks invariant observables of seismicity? In particular, can one define aftershocks without using space-time windows selected by the observer?

A quantitative metric of the correlation between any two earthquakes, or the extent to which one can be considered an aftershock of another, may be crucial for solving these problems, and for developing a better understanding of seismicity. Such a metric should include known statistical properties of seismicity that are robust with respect to the space-time window chosen by the observer (unlike previous methods of aftershock identification). One robust law is the Gutenberg-Richter (GR) distribution [4] for the number of earthquakes of magnitude m in a seismic region,

$$P(m) \sim 10^{-bm}, \tag{1}$$

with b usually ≈ 1. Another is the fractal appearance of earthquake epicenters [1,3,11], with fractal dimension d_f. These are both general statistical laws that hold over the entire Earth's surface, wherever earthquakes have been systematically collected. However, the observed exponents b and d_f may vary slightly depending on the seismic region and time span considered.

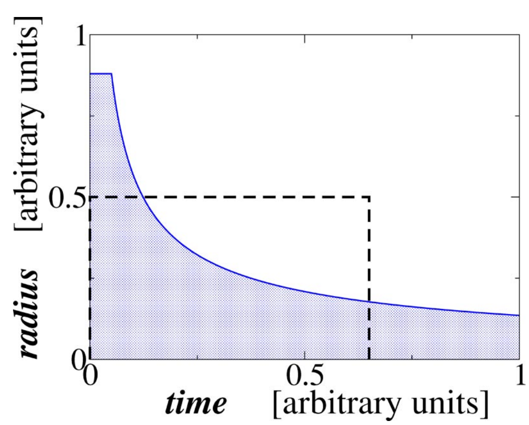

FIG. 1. (Color online) Schematic examples of space-time windows used to collect aftershocks: the usual rectangular or convex window (dashed line) and our hyperbolic, concave window (shaded region).

*Electronic address: maya@ic.ac.uk

Combining these two laws, the average number of earthquakes of magnitude within an interval Δm of m, occurring in an area of radius r over a time interval τ, is

$$\overline{n} = C\ \tau\, r^{d_f} \Delta m\ 10^{-bm}, \tag{2}$$

where C is a constant depending on the overall seismicity in the region and time interval under consideration.

For any earthquake j in the seismic region, looking backward in time, how many earthquakes of magnitude within an interval Δm of m would be expected to have occurred within a time interval t, and within a distance l, of that specific event? In fact, an n value can be defined between any two events i and j occurring in the sequence at times T_i and T_j, with $T_i < T_j$. If we take the magnitude m_i of the ith event, the spatial distance $l = l_{ij}$ between the two earthquake epicenters, and the time interval $t = t_{ij} = T_j - T_i$, the expected number of events of magnitude within Δm of m_i occurring in the particular space-time domain bounded by events j and i is

$$n_{ij} \equiv C t l^{d_f} \Delta m\ 10^{-bm_i}. \tag{3}$$

Note that the domain appearing in Eq. (3) is selected by the particular history of seismic activity in the region and not preordained by any observer.

Of all the earthquakes preceding j, the most unlikely to occur according to Eq. (3) is earthquake i^* such that n_{ij} is minimized when $i = i^*$. However, earthquake i^* *actually* occurred relative to j, even though it was the least likely to have done so. Therefore, i^* must be the event to which earthquake j is most correlated. In general, if $n_{ij} \ll 1$, then the correlation between j and i is very strong, and *vice versa*. By this argument, the correlation c_{ij} between any two earthquakes i and j is inversely proportional to n_{ij}, or

$$c_{ij} = 1/n_{ij}.$$

As we show later, the distribution of the correlation variables c_{ij} (or their inverse n_{ij}) for all pairs i,j is extremely broad. Therefore, for each earthquake j, a few exceptional events in its past have much larger correlation than all the others. (One of these will be the extremal event i^*.) These strongly correlated pairs of events can be marked as linked nodes, and the collection of linked nodes over all earthquakes forms a network.

The metric defined by Eq. (3) allows a classification of aftershocks. Further, the question of which is the better candidate to be the foreshock of an event can be quantitatively decided. Hierarchical clusters of earthquakes emerge, in which the biggest event in the cluster is called the main event, but where possibly later aftershocks create their own sequences of aftershocks, whenever they are able to “steal” aftershocks from the main event, and so on for further generations of aftershocks. Nevertheless, earthquakes are automatically collected into hierarchically self-organized clusters, or networks, without any special preanalysis of single event properties, or selection of space-time windows.

In the language of modern complex network theory [12,13], what we achieve is a time-oriented growing network where nodes (earthquakes) have internal variables (magnitude, occurrence time, and location), and links between the nodes carry a weight (the metric n_{ij} or its inverse c_{ij}) and are directed according to the time orientation, from the older to the newer nodes. Empirically, we find that both the distribution of outgoing links and the cluster size distribution are scale free. Due to the continuous nature of the link variable n_{ij}, no event is *a priori* purely an aftershock or a main shock. However, due to the broad distribution of n_{ij} observed, main shocks and aftershocks emerge as extreme limits of a continuous spectrum of the extent to which any given event can be considered to be a precursor or aftershock of other events in the sequence.

Since the space-time-magnitude scales appearing in Eq. (3) are selected by the actual sequence of events, the variables n_{ij} can be considered to be self-organizing tags of the underlying physical process governing seismicity. Note that singularities are eliminated by taking a small scale cutoff in time (here $t_{\min} = 180$ sec) and a minimum spatial resolution (here $l_{\min} = 100$ m).

Our approach was inspired by a recent analysis of earthquake waiting times by Bak *et al.* [6,14]. They introduced a space-time-magnitude scaling variable that allows a data collapse of the distribution of waiting times between subsequent earthquakes larger than a specified magnitude, occurring within grid cells of a specified size, covering nonoverlapping areas of the Earth. Also, Abe and Suzuki found scale-free networks for earthquakes in a completely different context, where nodes representing these grid cells were linked when subsequent earthquakes occurred in them [15]. However, neither of these works quantified the correlation between an arbitrary pair of earthquakes, or dealt with the subject of aftershock identification.

II. DATA AND PARAMETERS

The catalog we have analyzed is maintained by the Southern California Earthquake Data Center (it can be downloaded from the SCEDC web site http://www.scecdc.scec.org/ftp/catalogs/scsn), for which $\Delta m = 0.1$. It is considered to be complete for events with $m > 2$. We use data ranging from January 1, 1984 to December 31, 2000. In order to work with a well-defined ensemble, a lower threshold on the magnitude is introduced: events with magnitude smaller than $m_<$ are discarded. For each event, its position i in the sequence is used as a label, and we record the magnitude m_i, the occurrence time T_i (measured in seconds from midnight of the first day), and the latitude and longitude of the epicenter (converted to angles measured in radians, θ_i and ϕ_i, respectively). The distance between two events i and j is then measured as the arc length on the Earth’s surface, $l_{ij} = R_0 \arccos[\sin(\theta_i)\sin(\theta_j) + \cos(\theta_i)\cos(\theta_j)\cos(\phi_i - \phi_j)]$, where the Earth’s radius is $R_0 = 6.3673 \times 10^6$ m.

The b value of the GR law is $b \simeq 0.95$ for this data set, while $d_f \simeq 1.6$ was found by Corral [14] using a box counting procedure. It is consistent with the correlation dimension we measure for most of our clusters. However, many of the statistical results we find are not sensitive to the precise value of d_f or b.

With these units and values, the constant C can be estimated using Eq. (2). However, a precise evaluation of C is

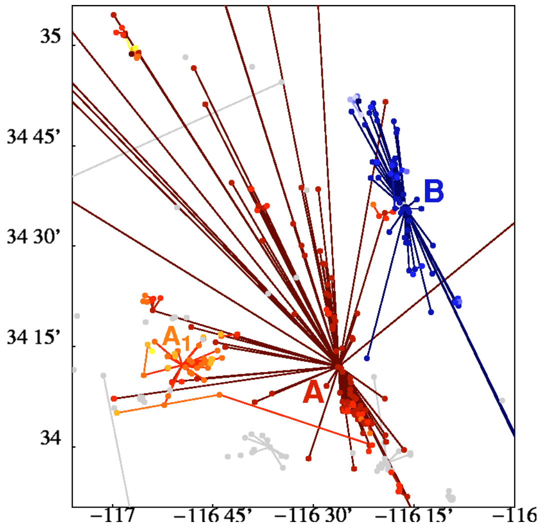

FIG. 2. (Color online) Scale-free earthquake network around Landers epicenter (cluster A, red online) and Hector Mine epicenter (cluster B, blue online). Colors fade with the aftershock generation, from darker to lighter within each cluster. Note that the big event following the Landers earthquake, giving rise to its own subcluster (A_1, orange online) of aftershocks, is not a first generation aftershock, since it has no link from Landers. Here $m_< = 4$ and $n_c = 10^{-2}$.

not possible, because $\overline{n}$ is the mean of a variable with huge variations in space and time. We have measured $\overline{n}$ for several circular windows well inside the zone covered by the catalog, finding $C \leqslant 10^{-9}$. For simplicity, our choice in this paper is $C = 10^{-9}$. Most of our results are insensitive to the precise value of C because we focus on relative, rather than absolute correlations between a pair of events. Throughout this paper we use, unless otherwise stated, the above mentioned values, and a lower threshold $m_< = 2.5$. For this value of $m_<$, the number of nodes in the network constructed using the entire catalog is $N = 28398$, while, e.g., for $m_< = 4$, as per Fig. 2, $N = 902$. Other than changing the cutoff where finite system size effects appear, the precise value of $m_< > 2$ has no effect on the statistical properties of the network we report here.

To simplify notation, we denote the probability distribution of a generic quantity q as $P(q)$. On finding distributions decaying as power laws, a clearer result appears by binning the values of $P(q)$ in properly normalized bins of a width that grows geometrically with q.

III. RESULTS

A part of the network constructed using this method is shown in Fig. 2. Hierarchically organized clusters of earthquakes emerge, where the links join aftershocks with their most correlated predecessor.

IV. EXPLANATION OF METHOD

Figure 3 shows the probability distribution of correlation values, $P(c)$, obtained by sampling over all earthquake pairs in the data set. It is an extremely broad distribution that

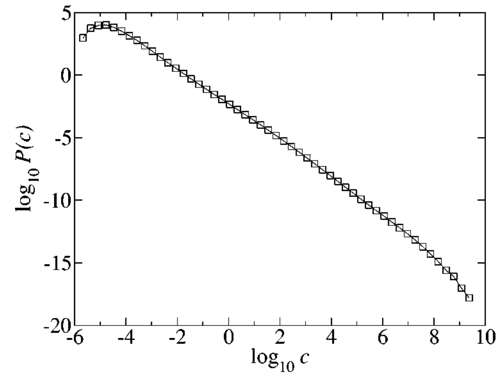

FIG. 3. The probability distribution of the correlation c between all earthquake pairs in the data base, with $m_< = 2.5$. It is a scale-free distribution over more than thirteen orders of magnitude.

exhibits power law behavior over more than 13 orders of magnitude:

$$P(c) \sim c^{-\tau} \quad \text{with} \quad \tau = 1.5 \pm 0.05. \tag{4}$$

Of course, the distribution of values $n = 1/c$ is also a power law $P(n) \sim n^{-\omega}$, with $\omega + \tau = 2$. In this case $\omega \approx 0.5$. Given such a broad distribution, for any earthquake j, a few extreme events i exist whose correlations c_{ij} are much larger than all the others. Therefore, it makes sense to represent these few earthquake pairs as nodes that are linked, while not linking pairs that have much smaller values of c_{ij}. Then the sequence of earthquakes may be usefully represented as a sparse network, where links exist between the most strongly correlated events. In the simplest implementation, earthquake j links solely to its *extremal predecessor* i^* which has the largest c_{ij}.

Constructing the extremal network, each new earthquake j attaches with a single link to the previous earthquake in the sequence that minimizes n_{ij} (or maximizes c_{ij}), with a weight denoted as n_j^*. Hence, each link carries the extremal n_j^* for the added node j relative to all previous nodes, and globally one obtains a growing directed tree. Links with small n_j^* indicate a stronger correlation between the emitting node and the receiving one, and are expected to identify events normally classified as aftershocks. Weak links with large n_j^* arise when none of the previous events are sufficiently strong, and close in space and time to event j. Clearly, the first earthquake in the time series has no incoming link.

A natural decomposition of the network into clusters is achieved by then removing all weak links where $n_j^* > n_c$, and n_c is a link threshold value. The correlated events are reliably detected when n_c is less than 1 but not extremely small. In the latter case, correlated events detach, and a very fragmented network appears. For large n_c some uncorrelated events make links, and a giant cluster appears. The resulting space-time windows are concave (see Fig. 1, and Conclusions), at variance with the convex windows usually used.

In order to quantitatively assess the properties of this network, we start by analyzing the distribution of link weights $P(n^*)$. This distribution exhibits power law behavior with an exponent $\simeq -1$ up to a cutoff, as shown in Fig. 4. The distri-

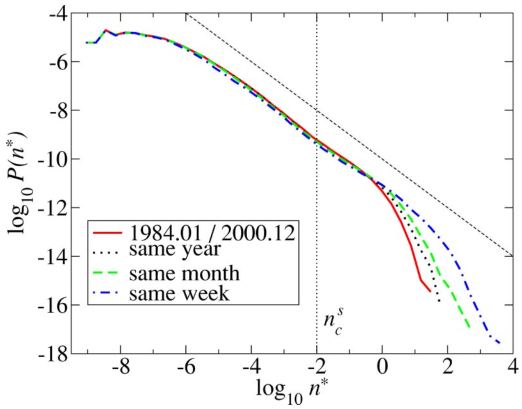

FIG. 4. (Color online) The distribution of link weights, n^*, for sequences of different temporal duration. An average over all nonoverlapping time intervals of the same duration is shown. The power law behavior is stable to variations in the duration. However, the cutoff moves to smaller n^* on increasing the measurement time interval as weakly linked earthquakes find more correlated predecessors further in the past. The vertical dotted line represents the estimated transition point, n_c^s, for the giant cluster. The straight dashed line has a slope −1.

bution of correlations between linked nodes in the extremal network $P(c^*)$ is also a power law, $P(c^*) \sim 1/c^*$. Such a broad, continuous distribution, without particular characteristic peaks, indicates that a division of earthquakes into rigid classes is intrinsically impossible. Instead, a continuum of possibilities ranges from clear aftershocks, which have an incoming link with small n^*, to events that are independent, with an incoming link of large n^*, but may emit many outgoing links with small n^*, and would be called main shocks.

A. The scale-free network

The resulting network of earthquakes is scale free. The number of aftershocks of an earthquake is equal to the number k of outgoing links from the node representing that event. In the language of network theory, this is called the outdegree of the node. Figure 5 shows that earthquakes in Southern California form a scale-free network, with an outdegree distribution scaling over more than three decades, with an index $\gamma = 2.0(1)$.

Recently, many scale-free networks with $P(k) \sim k^{-\gamma}$ have been discovered [12,13] in a broad variety of contexts. These include the Internet [16], the citation network, and the worldwide web [17], which are man-made; protein interaction and genetic regulatory networks [18,19], which are products of biological evolution; and the solar coronal magnetic field [20], which is physical network embedded in three-dimensional space formed by turbulent magnetohydrodynamic forces at very high magnetic Reynolds number. The aftershock network found here appears to be in a separate category from all previous examples. As we show later, many other characteristics, in addition to the out-degree distribution, of the aftershock network are scale-free—as demonstrated in, e.g., Figs. 4, 8, and 9. These other properties make it unlikely that the aftershock network can be described

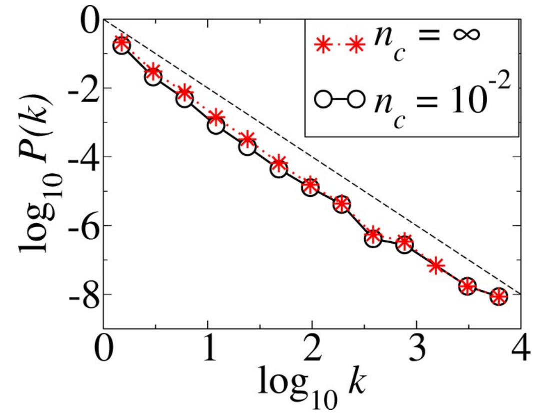

FIG. 5. (Color online) The degree distribution of the network of earthquakes and aftershocks. The out-degree k is the number of aftershocks linked to an earthquake. The introduction of a threshold n_c does not alter the observed behavior. The dashed line has slope −2, indicating a scale-free degree distribution $P(k) \sim k^{-\gamma}$ with $\gamma \approx 2$.

with a preferential attachment model or other model for scale-free networks discussed so far in the literature.

B. Clusters and the giant component

Lowering the link threshold n_c from infinity, the fully connected network breaks into clusters, in a percolationlike transition from a giant component to a finite cluster regime. As in percolation theory [21], the fraction of nodes in the biggest cluster (θ) is a good order parameter, displaying two distinct regimes, meeting at a point marked by an arrow in Fig. 6. Above $n_c = 10^{-1}$ in the phase with a giant component, θ grows quickly with n_c, while below $n_c = 10^{-2}$ in the finite cluster regime, it increases much more slowly with n_c. We estimate the transition to take place between $n_c = 10^{-1}$ and $n_c = 10^{-2}$. This estimate is consistent with that obtained by examining the distribution of cluster sizes N, which is the total number of earthquakes in a connected cluster, as a function of n_c (see Fig. 7). Near the transition, the cluster size

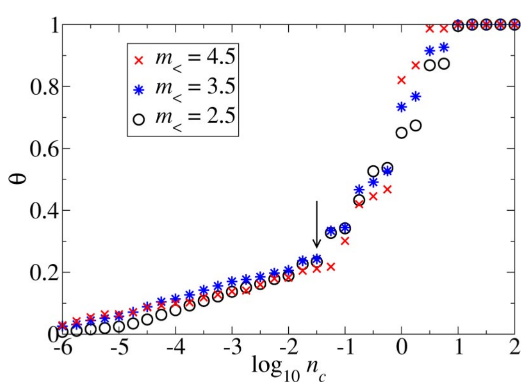

FIG. 6. (Color online) Order parameter for the percolationlike transition from a giant component to a finite cluster regime. Fraction of nodes in the biggest cluster as a function of the threshold n_c, for three values of $m_<$. The arrow marks the boundary between the two regimes we expect.

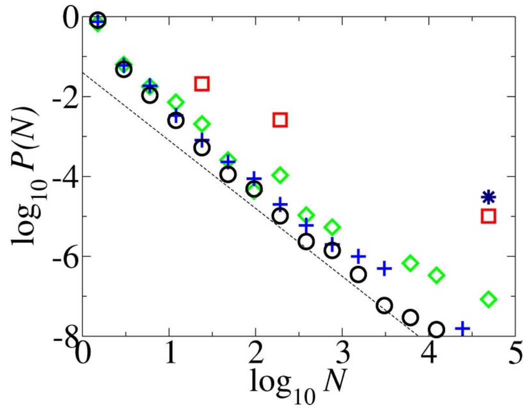

FIG. 7. (Color online) Cluster size distribution for different link thresholds. At large n_c, a giant cluster exists that is well separated in size from some remaining small ones. Between $n_c=10^{-1}$ and $n_c=10^{-2}$, an apparently continuous transition occurs where the finite cluster distribution extends out toward the giant cluster, and the distribution of cluster sizes exhibits power-law behavior. The straight line has a slope −1.7. Symbols are ($*, n_c=10^2$; $\square$, $n_c=10$; $\diamond$, $n_c=1$; $+$, $n_c=10^{-1}$; $\bigcirc$, $n_c=10^{-2}$).

distribution also appears to be scale-free, $P(N) \sim N^{-1.7(1)}$. Furthermore, a scaling regime exists for a wide range of link thresholds, indicating a relative insensitivity to a sharp separation between what are considered to be correlated and uncorrelated events. For clarity, we use the value $n_c^s=10^{-2}$ to locate the transition point where the giant component emerges. This value is consistent with our ansatz, Eq. (3), which requires that correlated events have n values significantly less than 1. Networks constructed with n_c^s therefore only link strongly correlated events. Obviously for networks the average number of outgoing links per node is equal to the

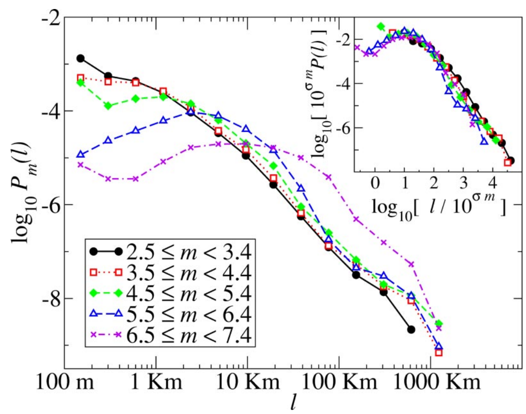

FIG. 8. (Color online) Link length distribution for different magnitudes of the emitting earthquake, at n_c^s. The length at maximum grows with magnitude roughly as $l_{\max} \sim 10^{0.4m}$, but the distributions have a fat tail, extending up to hundreds of kilometers even for intermediate magnitude events. These distributions are consistent with a hierarchical organization of events, where big earthquakes preferentially link at long distance with intermediate ones, which in turn link to more localized aftershocks, and so on. Inset: distributions rescaled according to Eq. (5) with $\sigma=0.4$.

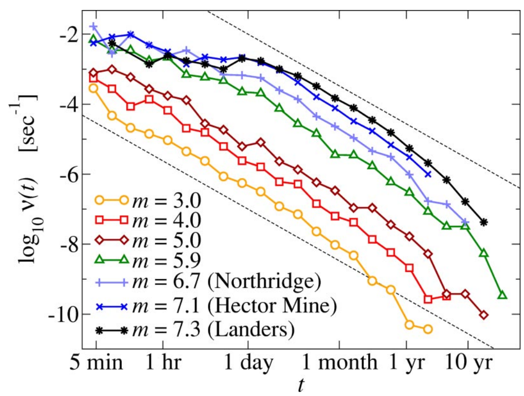

FIG. 9. (Color online) The Omori law for aftershock rates. These rates are measured for aftershocks linked to earthquakes of different magnitudes m using n_c^s. For each magnitude, the rate is consistent with the original Omori law, Eq. (6), up to a cutoff time that depends on m. As guides to the eye, dashed lines represent a decay $\sim 1/t$.

average number of incoming links; i.e., $\langle k_{\text{out}}\rangle = \langle k_{\text{in}}\rangle$. If $n_c=\infty$ then $\langle k_{\text{in}}\rangle=1$ (excluding the first earthquake), while for $n_c=10^{-2}$, $\langle k_{\text{in}}\rangle=0.7(1)$.

In Fig. 4, we study the effect of changing the temporal span of the catalog on the distribution of link weights. The power law behavior for strong links is stable, certainly up to n_c^s. However, the cutoff in $P(n^*)$ for weak links decreases to smaller n^* values, when earthquakes can link to events at further distance in the past. For an ideal "infinite" catalog, we conjecture that the cutoff value cannot be less than n_c^s.

C. Scaling law for aftershock distances

We define the link length l as the distance between the epicenter of an aftershock and its linked predecessor. The distribution of link lengths depends on the magnitude m of the predecessor, being on average greater for larger m. Dividing the link length distribution into classes depending on the magnitude of the predecessor, $P_m(l)$, a maximum in the distribution occurs, which shifts to larger l on increasing m, as shown in Fig. 8. This behavior is consistent with using larger space-time windows to collect aftershocks from larger events.

However, the distribution of link lengths exhibits no cutoff at large distances, but rather decays slowly as a power law with l, up to the linear extent of the seismic region covered by the catalog. The different distributions are consistent with a scaling ansatz:

$$P_m(l) \simeq 10^{-\sigma m} F(l/10^{\sigma m}), \qquad (5)$$

where l is measured in meters, $\sigma \approx 0.4$, and $F(x)$ is a scaling function. The tail of the scaling function is a power law; i.e., $F(x) \sim x^{-\lambda}$ with $\lambda \approx 2$ for $x \gg 1$. A data collapse using this ansatz is shown in the inset of Fig. 8. Such a slow decay at large distances calls into question the use of sharply defined space windows for collecting aftershocks, as already pointed out by Ogata [22].

D. The Omori law for earthquakes of all magnitudes

Figure 9 shows the rate of aftershocks for the Landers, Hector Mine, and Northridge events. Aftershocks occurring at time t after one of these events are binned into geometrically increasing time intervals. The number of aftershocks in each bin is then divided by the temporal width of the bin to obtain a rate of earthquakes per second. The same procedure is applied to each remaining event, not aftershocks of these three. An average is made for the rate of aftershocks linked to events having a magnitude within an interval Δm of m. Figure 9 also shows the averaged results for $m=3$ (1710 events), $m=4$ (161 events), $m=5$ (28 events), and $m=5.9$ (4 events).

The collection of aftershocks linked to earthquakes of all magnitudes is one of the main results of our method. Even intermediate magnitude events can have aftershocks that persist up to years. Earthquakes of all magnitudes have aftershocks which decay according to the Omori law [5,23],

$$\nu(t) \sim \frac{K}{c+t} \quad \text{for} \quad t < t_{\text{cutoff}}, \tag{6}$$

where c and K are constant in time, but depend on the magnitude m [23,24] of the earthquake. We find that the Omori law persists up to a time t_{cutoff} that also depends on m as well as the link threshold, n_c. Estimates of the cutoff times for n_c^s are $t_{\text{cutoff}} \approx 3$ months for $m=3$, and $t_{\text{cutoff}} \approx 1$ yr for $m=4$. For larger magnitudes, it is difficult to distinguish t_{cutoff} from the temporal duration of the data set.

The Omori law for aftershocks emerges as a result of our analysis, although it is not part of the original ansatz, Eq. (3), used to define aftershocks. It has been extensively investigated over decades, together with its modified version [23] involving a scaling $\sim t^{-p}$. The data shown in Fig. 9 are consistent with the original Omori result, $p=1$, for aftershocks of earthquakes of all magnitudes, once second and further generations of aftershocks are excluded. Our result is also consistent with theoretical studies on stick-slip motion [25,26], which suggest $p \approx 1$.

V. DISCUSSION

Convex space-time windows have been used since the 1970's [7–10], often with the size of the window determined by the main shock magnitude. The performance of this procedure is satisfactory for large earthquakes, although fixed window sizes may omit relevant aftershocks. Nevertheless, as a shortcoming, it can lead to distortions if many large aftershocks occur. In this case, nothing can be said on the "ownership" of further aftershocks.

Different approaches to the problem of aftershocks collection were proposed by several authors, sometimes with the aim to cure the former shortcomings. For a review see Ref. [27]. Our method has some similarities with these approaches. For instance, Frohlich and Davis collected earthquakes in clusters [28] by means of a different linking procedure. However, their analysis was done using a metric of the form $\sim\sqrt{l^2+\text{const}\, t^2}$, which does not take into account the magnitude of events, and has a space-time form at variance with measured earthquake correlations.

Maximum likelihood methods [29,30], in the context of seismicity, usually start with an ansatz on the law governing aftershocks, typically the modified Omori law. It is further assumed that seismicity is a nonstationary Poisson branching process. Models including these assumptions have been called epidemic type aftershock sequence models (ETAS, see Ref. [30]). Using a likelihood analysis with space, time, and magnitude, Ogata compared several forms of aftershocks distance distributions [22], and showed that an aftershock rate of the form

$$\nu_{m,l}(t) \sim \frac{10^{\alpha m}}{[c_l(m)+l]^{\mu}(c_t+t)^{p}} \tag{7}$$

was the most appropriate among his choices [c_t , α, p, and μ are constant, while $c_l(m)$ is scaling with the magnitude m of the main shock]. Hence, he also concluded that fixed space windows were not the best choice. Indeed, our metric variable n in Eq. (3) somewhat resembles his form of ν. The same form was also adopted in ETAS models [31–33]. In this framework, one has $\gamma=1+b/\alpha \gtrsim 2$ [33] and the exponent of the distribution of cluster sizes is $1+\gamma^{-1} \lesssim 2$. Both values are in agreement with our measurements of these exponents from the empirical data, using our metric ansatz together with the network construction. Thus ETAS models with an appropriately chosen ν give some results consistent with our findings.

However, our method is simpler to implement than likelihood methods. Furthermore, it does not require an ansatz on the validity of the modified Omori law, or on the type of statistical process that describes seismicity. Instead, the original Omori law is found as a result of our analysis. In addition, the physical argument leading to the variable n_{ij} also fixes the parameters in its definition, without the need to evaluate them by maximizing a likelihood. The only ansatz we make is the form of the metric.

One could object that the values of b and/or d_f can depend on the region of the Earth being considered, or may fluctuate depending on the specific fault zone being studied. However, the statistical results we find, as shown in the figures, are remarkably robust to variations in either of these parameters, or of the threshold $m_<$. Varying d_f over a wide range, from 1 to 3 (using $d_f > 2$ requires the introduction of event depths, see below) does not alter considerably the distribution of outgoing links, which retains its power law behavior with index $\gamma \approx 2$. The distribution of link weights, n^*, is even more insensitive to variations of b and d_f. Also the Omori law with $p \approx 1$, shown in Fig. 9, does not depend sensibly on the parameters, and holds for aftershocks linked to earthquakes of all magnitudes.

The crust of the Earth has a finite width ($\approx$20 km in California) in which events take place according to a "three-dimensional" fractal distribution, involving their depth. It is believed that there is a qualitative difference between small earthquakes and large ones, the former producing ruptures smaller that the crust width [2]. Hence, our arguments may need to be corrected at distances of the order of tens of kilometers. We have computed spatial distances through the three-dimensional Euclidean metric distance, using an appropriately revised d_f in Eq. (3). No significant departures from the results leading to our present conclusions were found.

Multiconnected networks

The introduction of more than one correlated predecessor for an event will be the subject of a future investigation. This is accomplished by attaching links between all earthquake pairs where $n_{ij} < n_c$. In this case, a general network, which is not treelike, emerges. The clustering of earthquakes could then be quantified in terms of the clustering coefficient of the nodes in the network [19,34]. In our view, an earthquake network with nodes having multiple incoming links represents a second order modeling of seismicity, the first being the simple tree structure we have presented here. In any case, it is unlikely that including links to more than one strongly correlated predecessor will change the scale-free character of the resulting network, although, of course, the network will no longer have a tree structure.

VI. CONCLUSIONS

We have introduced a metric to determine correlations between earthquakes that takes into account known statistical properties of seismicity. By means of an appealingly simple yet quantifiable procedure, networks of earthquakes and aftershocks emerge, where the number of aftershocks linked to any event is scale-free with an index $\gamma \approx 2$. The metric is constructed by looking backward in time from any particular event and calculating an expected number of events that would occur, compared to events that actually occurred. If this ratio is significantly less than 1, then the preceding event is correlated with the particular one. This is reminiscent of Kierkegaard's adage that life must be lived forward, but can only be understood backward.

Due to the form of the metric n measuring correlations, larger earthquakes collect aftershocks from larger space-time windows. From Eq. (3), these windows have a spatial radius varying with time as $r_i(T) = [n_c(T - T_i)^{-1} 10^{bm_i}]^{1/d_f}$. They span an hyperbolic space-time region (see Fig. 1), which is at variance with the usual "rectangular" or convex windows, of constant radius up to a finite time. In our method, at early times after an earthquake, its aftershock collection window is wider in space than it is at later times.

According to our metric, an earthquake can be correlated to an event very far away, if it occurs shortly after it. This is consistent with observations of "remote triggering" [35]. It is also consistent with the hypothesis that seismicity is a self-organized critical phenomenon [36–38]. In that case, some locations may be "on the edge of giving an earthquake" (or toppling, according to the sandpile paradigm), and even a small perturbation from an event far away could trigger them. However, we do not necessarily ascribe the correlations measured here to represent a usual cause and effect relationship. In the sandpile paradigm a completely insignificant event, like adding one grain of sand to an enormous pile, can trigger an arbitrarily large avalanche involving the whole system. Indeed, seismicity as one hierarchically correlated self-organized critical process, generates the scale-free network of earthquakes and aftershocks.

Our results also suggest that modern network theory may be a useful and illuminating way to approach the complexities of seismicity, including perhaps problems related to prediction. Our metric and network construction may also have applications to other phenomena with intermittent bursts such as, for instance, solar flares or even turbulence.

[1] D. Turcotte, *Fractals and Chaos in Geology and Geophysics*, 2nd ed. (Cambridge University Press, Cambridge, 1997).
[2] C. H. Scholz, *The Mechanics of Earthquakes and Faulting*, 2nd ed. (Cambridge University Press, Cambridge, 2002).
[3] Y. Y. Kagan, Physica D **77**, 160 (1994).
[4] B. Gutenberg and C. F. Richter, Geol. Soc. Am. Bull. **34**, 1 (1941), special papers.
[5] F. Omori, J. Coll. Sci. Imp. Univ. Tokyo **7**, 111 (1894).
[6] P. Bak, K. Christensen, L. Danon, and T. Scanlon, Phys. Rev. Lett. **88**, 178501 (2002).
[7] J. Gardner and L. Knopoff, Bull. Seismol. Soc. Am. **64**, 1363 (1974).
[8] V. Keilis-Borok, L. Knopoff, and I. Rotwain, Nature (London) **283**, 259 (1980).
[9] L. Knopoff, Y. Kagan, and R. Knopoff, Bull. Seismol. Soc. Am. **72**, 1663 (1982).
[10] L. Knopoff, Proc. Natl. Acad. Sci. U.S.A. **97**, 11 880 (2000).
[11] T. Hirata, J. Geophys. Res. **64**, 7507 (1989).
[12] R. Albert and A.-L. Barabási, Rev. Mod. Phys. **74**, 47 (2002).
[13] *Handbook of Graphs and Networks*, edited by S. Bornholdt and H. G. Schuster (Wiley-VCH, Weinheim, Germany, 2002).
[14] A. Corral, Phys. Rev. E **68**, 035102(R) (2003).
[15] S. Abe and N. Suzuki, Europhys. Lett. **65**, 581 (2004).
[16] M. Faloutsos, P. Faloutsos, and C. Faloutsos, Comput. Commun. Rev. **29**, 251 (1999).
[17] A.-L. Barabási and R. Albert, Science **286**, 509 (1999).
[18] A. Wagner, Mol. Biol. Evol. **18**, 1283 (2001).
[19] S. Maslov and K. Sneppen, Science **296**, 910 (2002).
[20] D. Hughes, M. Paczuski, R. O. Dendy, P. Helander, and K. G. McClements, Phys. Rev. Lett. **90**, 131101 (2003); D. Hughes and M. Paczuski, e-print astro-ph/0309230.
[21] D. Stauffer and A. Aharony, *Introduction to Percolation Theory* (Taylor and Francis, London, 1994).
[22] Y. Ogata, Ann. Inst. Stat. Math. **50**, 379 (1998).
[23] T. Utsu, Y. Ogata, and R. S. Matsu'ura, J. Phys. Earth **43**, 1 (1995).
[24] S. Lise, M. Paczuski, and A. L. Stella, e-print cond-mat/0403037.
[25] J. Dieterich, J. Geophys. Res., [Solid Earth] **99**, 2601 (1994).
[26] J. Gomberg, N. Beeler, and M. Blanpied, J. Geophys. Res., [Solid Earth] **105**, 7857 (2000).
[27] G. M. Molchan and O. E. Dmitrieva, Geophys. J. Int. **192**, 501 (1992).
[28] C. Frohlich and S. D. Davis, Geophys. J. Int. **100**, 19 (1990).

[29] Y. Y. Kagan, Geophys. J. Int. **106**, 135 (1991).
[30] Y. Ogata, Pure Appl. Geophys. **155**, 471 (1999).
[31] A. Helmstetter and D. Sornette, Phys. Rev. E **66**, 061104 (2002).
[32] A. Helmstetter and D. Sornette, J. Geophys. Res., [Solid Earth] **108**, 2457 (2003).
[33] A. Saichev, A. Helmstetter, and D. Sornette, e-print cond-mat/0305007 (2003).
[34] D. J. Watts and S. H. Strogatz, Nature (London) **393**, 440 (1998).
[35] D. P. Hill *et al.*, Science **260**, 1617 (1993).
[36] P. Bak and C. Tang, J. Geophys. Res., [Solid Earth] **94**, 15635 (1989).
[37] P. Bak, *How Nature Works: The Science of Self-Organized Criticality* (Copernicus, New York, 1996).
[38] D. L. Turcotte, Rep. Prog. Phys. **62**, 1377 (1999).